# APPLICATION OF KANTBP PROGRAM OF FINITE ELEMENT METHOD IN THE COUPLED-CHANNELS CALCULATIONS FOR HEAVY-ION FUSION REACTIONS*

S.I. Vinitsky[a,b], P.W. Wen[a,c], A.A. Gusev[a,d]
O. Chuluunbaatar[a,e], R.G. Nazmitdinov[a,d], A.K. Nasirov[a]
C.J. Lin[c,f], H.M. Jia[c], A. Góźdź[g]

[a]Joint Institute for Nuclear Research, 141980 Dubna, Russia
[b]Peoples Friendship University of Russia (RUDN University)
117198 Moscow, Russia
[c]China Institute of Atomic Energy, 102413 Beijing, China
[d]Dubna State University, 141982 Dubna, Russia
[e]Institute of Mathematics and Digital Technologies
Mongolian Academy of Sciences, 13330 Ulan-Bator, Mongolia
[f]Department of Physics, Guangxi Normal University, 541004 Guilin, China
[g]Institute of Physics, University of Maria Curie-Skłodowska, Lublin, Poland

*(Received January 29, 2020)*

We apply a new calculation scheme of a finite element method and upgraded program KANTBP in the coupled-channels calculations for heavy-ion fusion reactions. We diagonalize the matrix of close coupled effective potentials to formulate ingoing wave boundary conditions in point within a pocket of the potential well with a true set of thresholds. Efficiency of the proposed approach is shown by successfully described experimental data for the sub-barrier and above-barrier fusion cross section of some reaction systems.

DOI:10.5506/APhysPolBSupp.13.549

## 1. Introduction

In the coupling channel (CC) method, regular boundary conditions with an additional optical potential starting with [1–3] are used to describe sub-barrier and above-barrier reactions with heavy ions. An alternative method of the ingoing wave boundary conditions (IWBC) uses the real potentials

* Presented at the XXVI Nuclear Physics Workshop *Key problems of nuclear physics*, Kazimierz Dolny, Poland, September 24–29, 2019.

[4–8]. However, for the formulation of the Robin or third type boundary conditions with the correct set of threshold energies, a diagonalization of the channel coupling matrix of the effective potentials (CCMPs) at the internal point pocket of potential well is required [9, 10].

In the present paper, a fusion of two nuclei that occurs at strong coupling of their relative motion to surface vibrations is analyzed. To this aim, a new efficient finite element method (FEM), that improves the KANTBP code [11–14], is used to solve numerically CC equations with the IWBC formulated with the above diagonalization of the CCMPs. A comparison of the presented results with available experimental data demonstrates some advantages of the modified KANTBP code with respect to the modified Numerov method with the IWBC formulated without the diagonalization of the CCMPs, presented as the CCFULL code [7]. It is shown that the deep sub-barrier and above-barrier fusion cross sections of some reaction systems have been successfully described.

Structure of the paper is the following. In Section 2, we present diagonalization process of the IWBC. In Section 3, we describe procedure of calculations of the vibrational coupling matrix elements of effective potentials. In Section 4, we discuss our results of calculations of some sub-barrier fusion reactions. In Conclusion, we describe further applications of KANTBP codes.

## 2. The setting of the problem with diagonalization of IWBC

We will solve the CC equations in isocentrifugal approximation (neglecting the Coriolis coupling of relative and internal nuclear motion of two heavy ions) on interval $r \in (0, \infty)$ by reduction to the finite interval $r \in (r_{\min}, r_{\max})$

$$\sum_{n'=1}^{N} \left( \left( -\frac{\mathrm{d}^2}{\mathrm{d}r^2} - \tilde{E} \right) \delta_{nn'} + W_{nn'}(r) \right) \psi_{n'n_\mathrm{o}}(r) = 0\,. \tag{1}$$

Here, $\tilde{E} = \frac{2\mu E}{\hbar^2}$ is the center-of-mass energy, $n_\mathrm{o}$ is a number of the open entrance channel with a positive relative energy $k_{n_\mathrm{o}}^2 = E_{n_\mathrm{o}} = \tilde{E} - \epsilon_{n_\mathrm{o}} > 0$, $n_\mathrm{o} = 1, \ldots, N_\mathrm{o} \le N$, $\{\psi_{nn_\mathrm{o}}(r)\}_{n=1}^{N}$ are components of a desirable matrix solution, $W_{nn'}(r) = W_{n'n}(r)$ are elements of the CCMPs determined by

$$W_{nn'}(r) = \frac{2\mu}{\hbar^2} \left[ \left( \frac{l(l+1)\hbar^2}{2\mu r^2} + V_N^{(0)}(r) + \frac{Z_\mathrm{P} Z_\mathrm{T} e^2}{r} + \epsilon_n \right) \delta_{nn'} + V_{nn'}(r) \right]. \tag{2}$$

Here, $\mu = A_\mathrm{P} A_\mathrm{T}/(A_\mathrm{P} + A_\mathrm{T})$ is reduced mass of the target and the projectile with masses $A_\mathrm{T}$ and $A_\mathrm{P}$ and charges $Z_\mathrm{T}$ and $Z_\mathrm{P}$, respectively. The quantum number $l$ is orbital momentum of relative motion, $W_{nn'}(r \to \infty) = \epsilon_n \delta_{nn'}$ is a set $0 \le \epsilon_1 < \epsilon_2 < \ldots < \epsilon_N$ of eigenenergies in increasing order of the Hamiltonians of internal motion in the harmonic approximation [7, 8].

To formulate IWBC in the point $r = r_{\min}$ with the correct set of threshold energies, we will diagonalize the $N \times N$ matrix $\boldsymbol{W} \equiv \boldsymbol{W}(r_{\min})$ at $r = r_{\min}$

$$\boldsymbol{W}\boldsymbol{A} = \boldsymbol{A}\tilde{\boldsymbol{W}}\,, \qquad \left\{\tilde{\boldsymbol{W}}\right\}_{nm} = \delta_{nm}\tilde{W}_{mm}\,,$$

where $\boldsymbol{A} \equiv \boldsymbol{A}(r_{\min})$ is $N \times N$ matrix of eigenvectors and $\tilde{W}_{11} \le \tilde{W}_{22} \ldots \le \tilde{W}_{NN}$ are corresponding eigenvalues. In this case, the linear independent matrix solution $\{\phi_{nm}(r)\}_{n,m=1}^{N}$ of Eqs. (1) can be written in the form of

$$\phi_{nm}(r) = A_{nm}y_m(r)\,. \tag{3}$$

The functions $y_m(r)$ are solutions of the uncoupled equations

$$y_m''(r) + K_m^2 y_m(r) = 0\,, \qquad K_m^2 = \tilde{E} - \tilde{W}_{mm}\,.$$

In open channels at $K_m^2 > 0$, $m = 1, \ldots, M_{\rm o} \le N$ and in closed channels at $K_m^2 < 0$, $m = M_{\rm o}+1, \ldots, N$, the solutions $y_m(r)$, respectively, have the form of

$$y_m(r) = \frac{\exp(-\imath K_m r)}{\sqrt{K_m}}\,, \qquad y_m(r) = \frac{\exp(|K_m| r)}{\sqrt{K_m}}\,. \tag{4}$$

In this case, the matrix of the asymptotic solutions $\{\psi^{\rm as}_{nn_{\rm o}}(r)\}_{n=1}^{N}$ at $n_{\rm o} = 1, \ldots, N_{\rm o}$ of Eq. (2) expressed by the linear combinations of the linear independent solutions $\phi_{nm}(r)$ determined by Eqs. (3) and (4) is

$$\psi^{\rm as}_{nn_{\rm o}}(r) = \sum_{m=1}^{M_{\rm o}} \phi_{nm}(r)\hat{T}_{mn_{\rm o}} \equiv \sum_{m=1}^{M_{\rm o}} A_{nm}y_m(r)\hat{T}_{mn_{\rm o}}\,, \qquad r \le r_{\min}\,, \tag{5}$$

where $\hat{T}_{mn_{\rm o}} \equiv \hat{T}^{(l)}_{mn_{\rm o}}$ is the matrix of desirable partial transmission amplitudes with the correct set of threshold energies $K_m^2 > 0$, $m = 1, \ldots, M_{\rm o} \le N$ in exit open channels of the IWBC that is calculated by the KANTBP 3.0 code.

*Remark.* The above asymptotes differs from the asymptotes $\{\psi^{\rm as}_{nn_{\rm o}}(r)\}_{n=1}^{N}$ at $n_{\rm o} = 1, \ldots, \tilde{N}_{\rm o}$ of Eq. (1) subjected the IWBC without diagonalization the matrix $\boldsymbol{W} \equiv \boldsymbol{W}(r_{\min})$ at $r \le r_{\min}$ accepted in CCFULL code with the non-correct set of threshold energies $(k_n(r_{\min}))^2 = E - W_{nn}(r_{\min})$ counting on the diagonal elements $W_{nn}(r_{\min})$. The corresponding asymptotes for the open exit channels $(k_n(r_{\min}))^2 > 0$ at $n = 1, \ldots, \tilde{N}_{\rm o}$ and the closed exit channels $(k_n(r_{\min}))^2 \le 0$ $n = \tilde{N}_{\rm o}+1, \ldots N$ have the form of

$$\psi^{\rm as}_{nn_{\rm o}}(r) = \begin{cases} \exp(\imath k_n(r_{\min})r)\hat{T}_{nn_{\rm o}}\,, & k_n(r_{\min}) = \sqrt{E - W_{nn}(r_{\min})} > 0\,, \\ \exp(\kappa_n(r_{\min})r)\,, & \kappa_n(r_{\min}) = \sqrt{W_{nn}(r_{\min}) - E} > 0\,. \end{cases}$$

In Fig. 1 (right), we display two sets of the diagonal elements $\hbar^2 W_{nn}(r_{\min})/2\mu$ and the corresponding eigenvalues $\hbar^2 \tilde{W}_n(r_{\min})/2\mu$ that revival the increasing number $M_{\rm o} > \tilde{N}_{\rm o}$ of exit open channels in deep sub-barrier region of the energy $E$ of fusion reactions with the IWBC formulated after diagonalization of the matrix $\boldsymbol{W} \equiv \boldsymbol{W}(r_{\min})$.

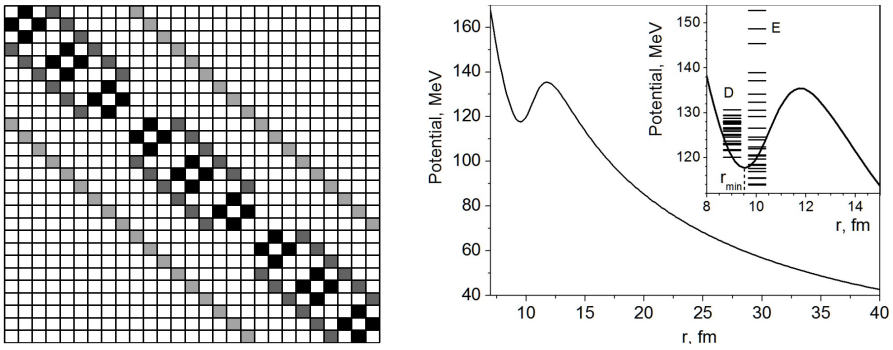


Fig. 1. Left: The structure of matrix $\hat{O}_{nm}(r)$ for $N_{T_{2^+}} = 2$, $N_{T_{3^-}} = 2$, $N_{P_{2^+}} = 2$ of vibration coupling. Right: The effective potential $V(r)$ (solid line), diagonal matrix elements of matrix $\boldsymbol{W}(r_{\min})$ (D) and eigenvalues of matrix $\boldsymbol{W}(r_{\min})$ (E) for the case of $^{32}$S+$^{182}$W.

At $r = r_{\max}$, the asymptotic solutions $\{\psi^{\rm as}_{nn_{\rm o}}(r)\}_{n=1}^{N}$ for $n_{\rm o} = 1, \ldots, N_{\rm o}$ of Eq. (1) are given in terms of the normalized outgoing and incoming Coulomb partial wave functions [15], $\hat{H}^{\pm}_l(k_n r) = H^{\pm}_l(k_n r)\exp(\mp i\sigma_l(k_n))$, where $\sigma_l(k_n)$ is the Coulomb phase, $H^{\pm}_l(k_n r) = (\pm iF_l(\eta_n, k_n r) + G_l(\eta_n, k_n r))/\sqrt{k_n}$, $k_n \geq 0$, $n = 1, \ldots, N_{\rm o} \leq N$, for open entrance channels and for components of $\psi^{\rm as}_{nn_{\rm o}}(r_{\max}) = o(1)$ with elements $n = N_{\rm o}+1, \ldots, N$ for closed entrance channels

$$\psi^{\rm as}_{nn_{\rm o}}(r) = \begin{cases} \hat{H}^{-}_l(k_n r)\delta_{n,n_{\rm o}} - \hat{H}^{+}_l(k_n r)\hat{R}_{nn_{\rm o}}\,, \\ 2|k_n|^{1/2} r^{l+1}\exp(-|k_n|r)U(l+1+\eta_n, 2l+2, 2|k_n|r)\,. \end{cases} \tag{6}$$

Here, $U(l+1+\eta_n, 2l+2, 2|k_n|r)$ is the Whittaker function [15], $\hat{R}_{nn_{\rm o}}$ are desirable partial reflection amplitudes, in particular, at $n_{\rm o} = 1$ from a ground state $|i_{\rm o}\rangle = |n_{\rm o} - 1\rangle = |0\rangle$ of the intrinsic motion before the collision. The Robin boundary conditions for the solutions $\psi_{nn_{\rm o}}(r)$ of Eq. (1) read as

$$\left(\frac{{\rm d}\psi_{nn_{\rm o}}(r)}{{\rm d}r} - \sum_{n'=1}^{N} G_{nn'}(r)\psi_{n'n_{\rm o}}(r)\right)_{r=r_{\min}, r_{\max}} = 0\,.$$

They are resolved by matching at $r = r_{\min}, r_{\max}$ the matrix $\{G_{nn'}(r)\}_{n,n'=1}^{N}$ of logarithmic derivatives of the numerical solutions $\psi_{nn_{\rm o}}(r)$ of Eq. (1) with

their asymptotic expansions $\psi^{\rm as}_{nn_{\rm o}}(r)$ from Eqs. (5) and (6), depending on unknown partial transition and reflection amplitudes $\hat{T}_{nn_{\rm o}}$ and $\hat{R}_{nn_{\rm o}}$, implemented in the KANTBP 3.0 code [11, 13]. The partial tunneling probability $P_l(E)$ from the entrance open channel $n_{\rm o}$, in particular, the ground state ($n_{\rm o} = 1$) is determined by the transmission coefficient

$$P_l(E) \equiv T^{(l)}_{n_{\rm o}n_{\rm o}}(E)\,.$$

Finally, the total fusion cross section is expressed as a sum over partial waves at the center-of-mass energy $E$, which is

$$\sigma_{\rm f}(E) \;=\; \sum_{l=0}^{L} \sigma^{(l)}_{\rm f}(E) = \frac{\pi}{k^2_{n_{\rm o}}} \sum_{l=0}^{L} (2l+1) P_l(E)\,.$$

At fixed orbital momentum $l$, it is given by summation over all possible intrinsic states of entrance $N_{\rm o}$ and exit $M_{\rm o}$ open channels

$$R^{(l)}_{n_{\rm o}n_{\rm o}}(E) = \sum_{n=1}^{N_{\rm o}} \left|\hat{R}_{nn_{\rm o}}\right|^2, \qquad T^{(l)}_{n_{\rm o}n_{\rm o}}(E) = \sum_{m=1}^{M_{\rm o}} \left|\hat{T}_{mn_{\rm o}}\right|^2,$$

where the relations $T^{(l)}_{n_{\rm o}n_{\rm o}}(E) = 1 - R^{(l)}_{n_{\rm o}n_{\rm o}}(E)$ take place. Note that the condition $T^{(l)}_{n_{\rm o}n_{\rm o}}(E) + R^{(l)}_{n_{\rm o}n_{\rm o}}(E) - 1 = 0$ fulfills with ten significant digits in calculations by means of the KANTBP code implemented FEM [11–13].

### *2.1. The vibrational coupling matrix elements of effective potentials*

To demonstrate working capacity of our approach, we analyze couplings of the relative motion to surface vibrations of a compound nucleus only, comparing our results with well-known results from literature. We consider a potential between the projectile and the target as a function of the relative distance $r$ between them

$$V(r) = V_{\mathcal{N}}(r) + V_{\rm C}(r)\,.$$

The potential contains the Coulomb term $V_{\rm C} = Z_{\rm P}Z_{\rm T}e^2/r$ and a phenomenological nuclear potential $V_{\mathcal{N}}(r)$ in the Woods–Saxon form

$$V_{\mathcal{N}}(r) = -\frac{V_0}{1 + \exp[(r - R_0)/a_0]}\,. \tag{7}$$

Here, the parameters $V_0$, $R_0$, $a_0$ are the potential depth, potential radius, and diffuseness, respectively, derived from the Akyüz–Winther (AW) parameterization [16] $V_0 = (16\pi\gamma a_0 \bar{R})$ MeV, $R_0 = R_{\rm P} + R_{\rm T}$, $\frac{1}{a_0} = 1.17[1 +$

$0.53(A_{\rm P}^{-1/3}+A_{\rm T}^{-1/3})]$ fm$^{-1}$, $\bar{R}=\frac{R_{\rm P}R_{\rm T}}{R_{\rm P}+R_{\rm T}}$, $R_i=(1.2A_i^{1/3}-0.09)$ fm, $i=P,T$, $\gamma=0.95\left(1-1.8\frac{(N_{\rm P}-Z_{\rm P})(N_{\rm T}-Z_{\rm T})}{A_{\rm P}A_{\rm T}}\right)$ MeV fm$^{-2}$. The coupling matrix elements $V_{nn'}(r)=V_{n'n}(r)$ in Eq. (2) are generated by changing the radius $R_0$ in the potential $V(r)$ to a dynamical operator $R_0+\hat{O}$ [17]

$$\hat{O}=\sum_{i={\rm T,P}}\sum_{\lambda_i}^{\lambda_i^{\max}}\frac{\beta_{\lambda_i}}{\sqrt{4\pi}}r_{\rm c}\,A_i^{1/3}\left(a^{\dagger}_{\lambda_i 0}+a_{\lambda_i 0}\right), \tag{8}$$

where $a^{\dagger}_{\lambda_i 0}$ ($a_{\lambda_i 0}$) is the creation (annihilation) operator of the vibrational mode of the multipolarity $\lambda$. In this representation, the matrix elements of the operator $\hat{O}$ between the vibrational states $|n\rangle=\prod_{i,\lambda_i}|n_{\lambda_i}\rangle$ and $|m\rangle=\prod_{j,\lambda_j}|m_{\lambda_j}\rangle$ at $i,j=P,T$ and $\lambda_i=2,\ldots,\lambda_i^{\max}$, $\lambda_j=2,\ldots,\lambda_j^{\max}$ read as

$$\hat{O}_{nm}=\sum_{i={\rm T,P}}\sum_{\lambda_i=2}^{\lambda_i^{\max}}\frac{\beta_{\lambda_i}r_{\rm c}\,A_i^{1/3}}{\sqrt{4\pi}}\left(\sqrt{m_{\lambda_i}}\delta_{n_{\lambda_i},m_{\lambda_i}-1}+\sqrt{n_{\lambda_i}}\delta_{n_{\lambda_i},m_{\lambda_i}+1}\right)\prod_{\lambda_j\neq\lambda_i}\delta_{n_{\lambda_j},m_{\lambda_j}},$$

where the $n_{\lambda_i}$-phonon or $m_{\lambda_j}$-phonon state of the multipolarity $\lambda_i$ or $\lambda_j$ is defined as [8]

$$|n_{\lambda_i}\rangle=\frac{1}{\sqrt{n_{\lambda_i}!}}\left(a^{\dagger}_{\lambda_i 0}\right)^{n_{\lambda_i}}|0\rangle, \qquad |m_{\lambda_j}\rangle=\frac{1}{\sqrt{m_{\lambda_j}!}}\left(a^{\dagger}_{\lambda_j 0}\right)^{m_{\lambda_j}}|0\rangle.$$

The deformation parameter $\beta_{\lambda_i}$, that defines the amplitude of the zero-point motion, can be determined from the experimental transition probability

$$\beta_{\lambda_i}=\frac{4\pi}{3Z_iR_i^{\lambda_i}}\sqrt{\frac{B(E\lambda_i)\uparrow}{e^2}},$$

where $R_i$, $i=P,T$ is the radius of the spherical nucleus. The adopted structure properties including excitation energies, deformation parameters for the nuclei used in this study are listed in [18, 19]. The low-lying collective $2^+$ and $3^-$ vibrational states are considered. The radius parameter $r_{\rm c}$ in the coupling interactions of Eq. (8) is assumed as 1.2 fm for both target and projectile in all the following calculations. The numbers of the target $3^-$ phonon, the target $2^+$ phonon and the projectile $2^+$ phonon are denoted as $N_{\rm T_{3^-}}$, $N_{\rm T_{2^+}}$, and $N_{\rm P_{2^+}}$, respectively. The total CC number will be $N_{\rm c}=(N_{\rm T_{3^-}}+1)(N_{\rm T_{2^+}}+1)(N_{\rm P_{2^+}}+1)-1$ when all the mutual excitations are included. It means that the number of coupled equations in Eq. (1) is equal to $N=N_{\rm c}+1$. We need the matrix elements $V_{nn'}(r)$ of the coupling between the vibrational states $|n\rangle$ and $|m\rangle$ of the target and projectiles listed

in Table I. The nuclear coupling matrix elements $V_{nm}^{(\mathcal{N})}(r)$ are calculated using the eigenvalues $O_\alpha$ and eigenvectors $\langle m|\alpha\rangle$ of the matrix $\hat{O}_{nm}$ having the band structure shown in Fig. 1 (left), *i.e.* solutions of the algebraic eigenvalues problem

$$\sum_{m=1}^{N}\left(\hat{O}_{nm}-O_\alpha\delta_{nm}\right)\langle m|\alpha\rangle=0\,.$$

The nuclear coupling matrix elements $V_{nm}^{(\mathcal{N})}(r)$ are then

$$V_{nm}^{(\mathcal{N})}(r)=\sum_{\alpha=1}^{N}\langle n|\alpha\rangle\langle\alpha|m\rangle V_{\mathcal{N}}(r,O_\alpha)-V_{\mathcal{N}}^{(0)}(r)\delta_{n,m}\,.$$

The term $V_{\mathcal{N}}^{(0)}(r)\equiv V_{\mathcal{N}}(r)$ counteracts the coupling interaction in the entrance channel. The linear coupling approximation for the Coulomb coupling $V_{nm}^{\mathrm{C}}(r)$ of the vibrational degree of freedom is taking into account [7]

$$V_{nm}^{\mathrm{C}}(r)=\sum_{i=T,P}\sum_{\lambda_i=2}^{\lambda_i^{\max}}f_i^{\lambda_i}(r)\left(\sqrt{m_{\lambda_i}}\delta_{n_{\lambda_i},m_{\lambda_i}-1}+\sqrt{n_{\lambda_i}}\delta_{n_{\lambda_i},m_{\lambda_i}+1}\right)\prod_{\lambda_j\neq\lambda_i}\delta_{n_{\lambda_j},m_{\lambda_j}},$$

where $f_i^{\lambda_i}(r)=\beta_{\lambda_i}/(4\pi)3Z_{\mathrm{P}}Z_{\mathrm{T}}e^2/(2\lambda_i+1)R_i^{\lambda_i}/r^{\lambda_i+1}$. The total coupling matrix element $V_{nm}(r)$ is given by the sum of $V_{nm}(r)=V_{nm}^{(\mathcal{N})}(r)+V_{nm}^{C}(r)$.

TABLE I

The list of the 27 CC for $N_{\mathrm{T}_{3^-}}=2$, $N_{\mathrm{T}_{2^+}}=2$, $N_{\mathrm{P}_{2^+}}=2$ in the form of $|n\rangle=|\mathrm{T}_{3^-}\mathrm{T}_{2^+}\mathrm{P}_{2^+}\rangle$ including the ground-state channel $|0\rangle=|000\rangle$. Non-marked are mutual states, the target and projectile states are marked by * and **, respectively.

| | | | | | | | | |
|---|---|---|---|---|---|---|---|---|
| 0 | 1 | 2 | 3 | 4 | 5 | 6 | 7 | 8 |
| $\|000\rangle$ | $\|100\rangle^*$ | $\|200\rangle^*$ | $\|010\rangle^*$ | $\|110\rangle^*$ | $\|210\rangle^*$ | $\|020\rangle^*$ | $\|120\rangle^*$ | $\|220\rangle^*$ |
| 9 | 10 | 11 | 12 | 13 | 14 | 15 | 16 | 17 |
| $\|001\rangle^{**}$ | $\|101\rangle$ | $\|201\rangle$ | $\|011\rangle$ | $\|111\rangle$ | $\|211\rangle$ | $\|021\rangle$ | $\|121\rangle$ | $\|221\rangle$ |
| 18 | 19 | 20 | 21 | 22 | 23 | 24 | 25 | 26 |
| $\|002\rangle^{**}$ | $\|102\rangle$ | $\|202\rangle$ | $\|012\rangle$ | $\|112\rangle$ | $\|212\rangle$ | $\|022\rangle$ | $\|122\rangle$ | $\|222\rangle$ |

### 3. Results of calculations of fusion reactions

In the following, we will examine two fusion reactions including $^{32}$S+$^{182}$W, and $^{28}$Si+$^{178}$Hf. The standard Akyüz–Winther-type Woods–Saxon potential mentioned above is adopted. Collective vibrations corresponding to $N_{T_{3-}} = 2$, $N_{T_{2+}} = 2$, and $N_{P_{2+}} = 2$ are included. There are totally 26 coupled channels. As mentioned above, we have shown the potential $V(r)$ for fusion reaction $^{32}$S+$^{182}$W at zero angular momentum in Fig. 1 (right). In order to clarify the role of the diagonalization procedure in the left boundary, the values $\hbar^2\tilde{\boldsymbol{W}}_n/2\mu$ (labeled E) and $\hbar^2\boldsymbol{W}_{nn}/2\mu$ (labeled D) are also indicated in this figure. For this fusion reaction, it can be seen that $\hbar^2\tilde{\boldsymbol{W}}_n/2\mu$ spreads much wider than $\hbar^2\boldsymbol{W}_{nn}/2\mu$. This demonstrates the significance of the non-diagonal elements. By considering these elements, the threshold changed a lot, as well as the number of open channels and closed channels. This will change the tunneling probability and the fusion cross section a lot.

The fusion cross sections for fusion reaction $^{32}$S+$^{182}$W and $^{28}$Si+$^{178}$Hf at the linear and logarithmic scales are presented in Fig. 2 (left) and Fig. 2 (right), respectively. The experimental data are taken from Ref. [21] for $^{32}$S+$^{182}$W, and Ref. [22] for $^{28}$Si+$^{178}$Hf. The predictions by KANTBP and the modified Numerov method (MNumerov) are shown as the solid and dashed lines. From this figure, it can be seen that the sub-barrier predictions

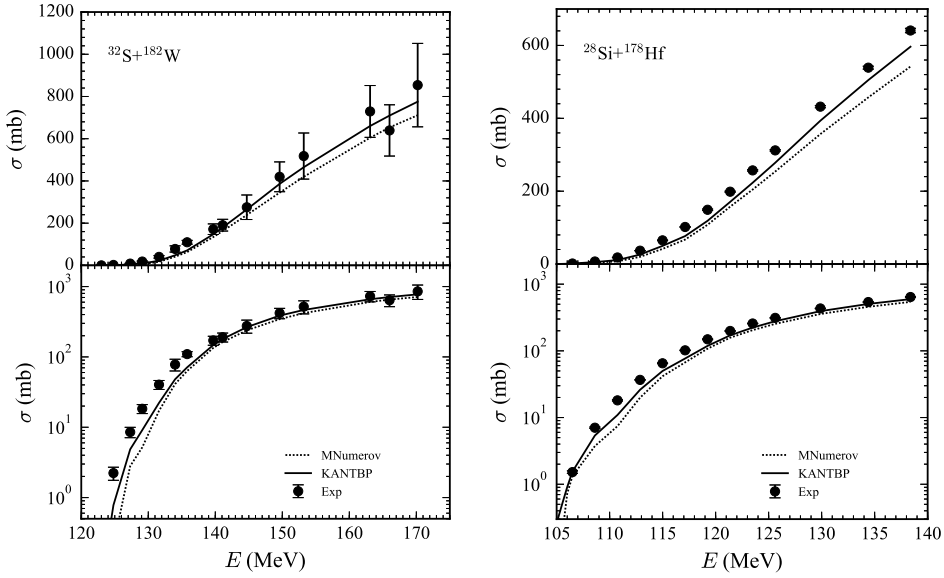


Fig. 2. Left: Fusion cross sections for fusion reaction $^{32}$S+$^{182}$W. Right: Fusion cross sections for fusion reaction $^{28}$Si+$^{178}$Hf. The experimental data (Exp, solid circles) are taken from Ref. [21] for $^{32}$S+$^{182}$W, and Ref. [22] for $^{28}$Si+$^{178}$Hf.

with diagonalization procedure (KANTBP) are generally more stable than that with the original boundary condition (MNumerov) at the left boundary. This is because the non-diagonal elements have been considered in this newly developed method, and there are less sudden non-continuous changes for wave functions.

In the left and right upper panels of Fig. 2, from the fusion cross sections at the linear scales for these two reactions, we can see that the predictions of the cross section with diagonalization are generally higher at all energy region for these two cases. That with diagonalization agrees with experimental data better with the standard Akyüz–Winther-type Woods–Saxon potential at both above-barrier and sub-barrier energy. The increase of the fusion cross sections is due to that shown in Fig. 1 (right). The threshold $\hbar^2\tilde{\boldsymbol{W}}_n/2\mu$ spreads much wider than $\hbar^2\boldsymbol{W}_{nn}/2\mu$. Especially, the minimum value of $\hbar^2\tilde{\boldsymbol{W}}_n/2\mu$ is obviously much lower. This is equivalent to the increase of the energy gap between incident energy and the minimum energy, which will increase the number of effective angular momentum. As a result, this causes the increase of the fusion cross sections, which is helpful to understand the diffuseness parameter anomaly problem [23].

## 4. Conclusion

The upgrade of KANTBP 3.0 [12] and next version KANTBP 4M program implemented in MAPLE are given in program library JINRLIB [14] for solutions to a given accuracy of multichannel scattering, eigenvalue and metastable state problems for the system of ODEs of the second order with continuous or piecewise continuous real or complex-valued coefficients.

Discretization of the boundary problems are implemented by the FEM with the interpolation Lagrange polynomials in KANTBP 3.0, and Hermite polynomials in KANTBP 4 preserves the property of continuity of derivatives of the desired solutions.

For a reduction of the scattering problem with a different number of open channels in the two asymptotic regions to the boundary problems on a finite interval, the asymptotic boundary conditions are approximately the homogeneous non-diagonal Robin or third-type boundary conditions.

The developed approach and codes provide useful tools for the CC calculations in heavy-ion fusion reactions. Since the explanations of experimental data are sensitive to the theoretical calculation, this study offers new insight into the understanding of the diffuseness parameter anomaly problem. We will show its impact on other phenomena such as on the deep sub-barrier hindrance phenomenon in our following works.

The authors thank to Profs. N.V. Antonenko and Zhigang Ge for useful discussions and support of this work. The work of P.W.W., C.J.L. and H.M.J. is supported by the National Key R&D Program of China (contract No. 2018YFA0404404), the National Natural Science Foundation of China (grants Nos. 11635015, 11805120, 11635003, 11805280, 11811530071, U1867212 and U1732145), and the Continuous Basic Scientific Research Project (No. WDJC-2019-13). A.K.N. thanks the RFBR for the partial support of the Joint DST-RFBR projects 17-52-45037 and 17-52-12015. The research benefited from computing of the HybriLIT heterogeneous platform of the JINR. This work was supported by the Polish–French COPIN collaboration of the project 04-113, Bogoliubov–Infeld and Hulubei–Meshcheryakov JINR programs, the grant RFBR and MECSS 20-51-44001, RUDN University Program 5-100 and grant of Plenipotentiary of the Republic of Kazakhstan in JINR.

## REFERENCES

[1] K. Tamura, *Rev. Mod. Phys.* **37**, 679 (1965).
[2] C.J. Lin, «Heavy-ion Nuclear Reactions», *Harbin Eng. Univ. Press*, Harbin 2015.
[3] B.B. Back *et al.*, *Rev. Mod. Phys.* **86**, 317 (2014).
[4] G.H. Rawitscher, *Nucl. Phys.* **85**, 337 (1966).
[5] P.R. Christensen, Z.E. Switkowski, *Nucl. Phys. A* **280**, 205 (1977).
[6] H.J. Krappe *et al.*, *Z. Phys. A.* **314**, 23 (1983).
[7] K. Hagino *et al.*, *Comput. Phys. Commun.* **123**, 143 (1999).
[8] K. Hagino, N. Takigawa, *Prog. Theor. Phys.* **128**, 1061 (2012).
[9] V.V. Samarin, V.I. Zagrebaev, *Nucl. Phys. A* **734**, E9 (2004).
[10] V.I. Zagrebaev, V.V. Samarin, *Phys. Atom. Nucl.* **67**, 1462 (2004).
[11] O. Chuluunbaatar *et al.*, *Comput. Phys. Commun.* **177**, 649 (2007).
[12] A.A. Gusev *et al.*, *Comput. Phys. Commun.* **185**, 3341 (2014).
[13] A.A. Gusev *et al.*, *Math. Model. Geom.* **3**, 22 (2015).
[14] https://www1.jinr.ru/programs/jinrlib/kantbp4m/indexe.html
[15] M. Abramowitz, I.A. Stegun, «Handbook of Mathematical Functions», Dover, NY 1965.
[16] A. Winther, *Nucl. Phys. A* **594**, 203 (1995).
[17] A. Bohr, B.R. Mottelson, «Nuclear Structure. Vol. II», Amsterdam 1974.
[18] S. Raman *et al.*, *Atom. Data. Nucl. Data. Tables* **78**, 1 (2001).
[19] T. Kibédi, R.H. Spear, *Atom. Data. Nucl. Data. Tables* **80**, 35 (2002).
[20] K. Hagino *et al.*, *Phys. Rev. C* **55**, 276 (1997).
[21] S. Mitsuoka, H. Ikezoe, K. Nishio, J. Lu, *Phys. Rev. C* **62**, 054603 (2000).
[22] R.D. Butt *et al.*, *Phys. Rev. C* **66**, 044601 (2002).
[23] J.O. Newton *et al.*, *Phys. Lett. B* **586**, 219 (2004).